

A study of the associated production of photons and b -quark jets in $p\bar{p}$ collisions at $\sqrt{s} = 1.96$ TeV

T. Aaltonen,²⁴ J. Adelman,¹⁴ B. Álvarez González^v,¹² S. Amerio^{dd},⁴⁴ D. Amidei,³⁵ A. Anastassov,³⁹ A. Annovi,²⁰ J. Antos,¹⁵ G. Apollinari,¹⁸ A. Apresyan,⁴⁹ T. Arisawa,⁵⁸ A. Artikov,¹⁶ J. Asaadi,⁵⁴ W. Ashmanskas,¹⁸ A. Attal,⁴ A. Aurisano,⁵⁴ F. Azfar,⁴³ W. Badgett,¹⁸ A. Barbaro-Galtieri,²⁹ V.E. Barnes,⁴⁹ B.A. Barnett,²⁶ P. Barria^{ff},⁴⁷ P. Bartos,¹⁵ G. Bauer,³³ P.-H. Beauchemin,³⁴ F. Bedeschi,⁴⁷ D. Beecher,³¹ S. Behari,²⁶ G. Bellettini^{ee},⁴⁷ J. Bellinger,⁶⁰ D. Benjamin,¹⁷ A. Beretvas,¹⁸ A. Bhatti,⁵¹ M. Binkley,¹⁸ D. Bisello^{dd},⁴⁴ I. Bizjak^{jj},³¹ R.E. Blair,² C. Blocker,⁷ B. Blumenfeld,²⁶ A. Bocci,¹⁷ A. Bodek,⁵⁰ V. Boisvert,⁵⁰ D. Bortoletto,⁴⁹ J. Boudreau,⁴⁸ A. Boveia,¹¹ B. Brau^a,¹¹ A. Bridgeman,²⁵ L. Brigliadori^{cc},⁶ C. Bromberg,³⁶ E. Brubaker,¹⁴ J. Budagov,¹⁶ H.S. Budd,⁵⁰ S. Budd,²⁵ K. Burkett,¹⁸ G. Busetto^{dd},⁴⁴ P. Bussey,²² A. Buzatu,³⁴ K. L. Byrum,² S. Cabrera^x,¹⁷ C. Calancha,³² S. Camarda,⁴ M. Campanelli,³¹ M. Campbell,³⁵ F. Canelli¹⁴,¹⁸ A. Canepa,⁴⁶ B. Carls,²⁵ D. Carlsmith,⁶⁰ R. Carosi,⁴⁷ S. Carrilloⁿ,¹⁹ S. Carron,¹⁸ B. Casal,¹² M. Casarsa,¹⁸ A. Castro^{cc},⁶ P. Catastini^{ff},⁴⁷ D. Cauz,⁵⁵ V. Cavaliere^{ff},⁴⁷ M. Cavalli-Sforza,⁴ A. Cerri,²⁹ L. Cerrito^q,³¹ S.H. Chang,²⁸ Y.C. Chen,¹ M. Chertok,⁸ G. Chiarelli,⁴⁷ G. Chlachidze,¹⁸ F. Chlebana,¹⁸ K. Cho,²⁸ D. Chokheli,¹⁶ J.P. Chou,²³ K. Chung^o,¹⁸ W.H. Chung,⁶⁰ Y.S. Chung,⁵⁰ T. Chwalek,²⁷ C.I. Ciobanu,⁴⁵ M.A. Ciocci^{ff},⁴⁷ A. Clark,²¹ D. Clark,⁷ G. Compostella,⁴⁴ M.E. Convery,¹⁸ J. Conway,⁸ M. Corbo,⁴⁵ M. Cordelli,²⁰ C.A. Cox,⁸ D.J. Cox,⁸ F. Crescioli^{ee},⁴⁷ C. Cuenca Almenar,⁶¹ J. Cuevas^v,¹² R. Culbertson,¹⁸ J.C. Cully,³⁵ D. Dagenhart,¹⁸ M. Datta,¹⁸ T. Davies,²² P. de Barbaro,⁵⁰ S. De Cecco,⁵² A. Deisher,²⁹ G. De Lorenzo,⁴ M. Dell'Orso^{ee},⁴⁷ C. Deluca,⁴ L. Demortier,⁵¹ J. Deng^f,¹⁷ M. Deninno,⁶ M. d'Errico^{dd},⁴⁴ A. Di Canto^{ee},⁴⁷ G.P. di Giovanni,⁴⁵ B. Di Ruzza,⁴⁷ J.R. Dittmann,⁵ M. D'Onofrio,⁴ S. Donati^{ee},⁴⁷ P. Dong,¹⁸ T. Dorigo,⁴⁴ S. Dube,⁵³ K. Ebina,⁵⁸ A. Elagin,⁵⁴ R. Erbacher,⁸ D. Errede,²⁵ S. Errede,²⁵ N. Ershaidat^{bb},⁴⁵ R. Eusebi,⁵⁴ H.C. Fang,²⁹ S. Farrington,⁴³ W.T. Fedorko,¹⁴ R.G. Feild,⁶¹ M. Feindt,²⁷ J.P. Fernandez,³² C. Ferrazza^{gg},⁴⁷ R. Field,¹⁹ G. Flanagan^s,⁴⁹ R. Forrest,⁸ M.J. Frank,⁵ M. Franklin,²³ J.C. Freeman,¹⁸ I. Furic,¹⁹ M. Gallinaro,⁵¹ J. Galyardt,¹³ F. Garbersson,¹¹ J.E. Garcia,²¹ A.F. Garfinkel,⁴⁹ P. Garosi^{ff},⁴⁷ H. Gerberich,²⁵ D. Gerdes,³⁵ A. Gessler,²⁷ S. Giagu^{hh},⁵² V. Giakoumopoulou,³ P. Giannetti,⁴⁷ K. Gibson,⁴⁸ J.L. Gimmell,⁵⁰ C.M. Ginsburg,¹⁸ N. Giokaris,³ M. Giordaniⁱⁱ,⁵⁵ P. Giromini,²⁰ M. Giunta,⁴⁷ G. Giurgiu,²⁶ V. Glagolev,¹⁶ D. Glenzinski,¹⁸ M. Gold,³⁸ N. Goldschmidt,¹⁹ A. Golossanov,¹⁸ G. Gomez,¹² G. Gomez-Ceballos,³³ M. Goncharov,³³ O. González,³² I. Gorelov,³⁸ A.T. Goshaw,¹⁷ K. Goulianos,⁵¹ A. Gresele^{dd},⁴⁴ S. Grinstein,⁴ C. Grosso-Pilcher,¹⁴ R.C. Group,¹⁸ U. Grundler,²⁵ J. Guimaraes da Costa,²³ Z. Gunay-Unalan,³⁶ C. Haber,²⁹ S.R. Hahn,¹⁸ E. Halkiadakis,⁵³ B.-Y. Han,⁵⁰ J.Y. Han,⁵⁰ F. Happacher,²⁰ K. Hara,⁵⁶ D. Hare,⁵³ M. Hare,⁵⁷ R.F. Harr,⁵⁹ M. Hartz,⁴⁸ K. Hatakeyama,⁵ C. Hays,⁴³ M. Heck,²⁷ J. Heinrich,⁴⁶ M. Herndon,⁶⁰ J. Heuser,²⁷ S. Hewamanage,⁵ D. Hidas,⁵³ C.S. Hill^c,¹¹ D. Hirschbuehl,²⁷ A. Hocker,¹⁸ S. Hou,¹ M. Houlden,³⁰ S.-C. Hsu,²⁹ R.E. Hughes,⁴⁰ M. Hurwitz,¹⁴ U. Husemann,⁶¹ M. Hussein,³⁶ J. Huston,³⁶ J. Incandela,¹¹ G. Introzzi,⁴⁷ M. Iori^{hh},⁵² A. Ivanov^p,⁸ E. James,¹⁸ D. Jang,¹³ B. Jayatilaka,¹⁷ E.J. Jeon,²⁸ M.K. Jha,⁶ S. Jindariani,¹⁸ W. Johnson,⁸ M. Jones,⁴⁹ K.K. Joo,²⁸ S.Y. Jun,¹³ J.E. Jung,²⁸ T.R. Junk,¹⁸ T. Kamon,⁵⁴ D. Kar,¹⁹ P.E. Karchin,⁵⁹ Y. Kato^m,⁴² R. Kephart,¹⁸ W. Ketchum,¹⁴ J. Keung,⁴⁶ V. Khotilovich,⁵⁴ B. Kilminster,¹⁸ D.H. Kim,²⁸ H.S. Kim,²⁸ H.W. Kim,²⁸ J.E. Kim,²⁸ M.J. Kim,²⁰ S.B. Kim,²⁸ S.H. Kim,⁵⁶ Y.K. Kim,¹⁴ N. Kimura,⁵⁸ L. Kirsch,⁷ S. Klimenko,¹⁹ K. Kondo,⁵⁸ D.J. Kong,²⁸ J. Konigsberg,¹⁹ A. Korytov,¹⁹ A.V. Kotwal,¹⁷ M. Kreps,²⁷ J. Kroll,⁴⁶ D. Krop,¹⁴ N. Krumnack,⁵ M. Kruse,¹⁷ V. Krutelyov,¹¹ T. Kuhr,²⁷ N.P. Kulkarni,⁵⁹ M. Kurata,⁵⁶ S. Kwang,¹⁴ A.T. Laasanen,⁴⁹ S. Lami,⁴⁷ S. Lammel,¹⁸ M. Lancaster,³¹ R.L. Lander,⁸ K. Lannon^u,⁴⁰ A. Lath,⁵³ G. Latino^{ff},⁴⁷ I. Lazzizzera^{dd},⁴⁴ T. LeCompte,² E. Lee,⁵⁴ H.S. Lee,¹⁴ J.S. Lee,²⁸ S.W. Lee^w,⁵⁴ S. Leone,⁴⁷ J.D. Lewis,¹⁸ C.-J. Lin,²⁹ J. Linacre,⁴³ M. Lindgren,¹⁸ E. Lipeles,⁴⁶ A. Lister,²¹ D.O. Litvintsev,¹⁸ C. Liu,⁴⁸ T. Liu,¹⁸ N.S. Lockyer,⁴⁶ A. Loginov,⁶¹ L. Lovas,¹⁵ D. Lucchesi^{dd},⁴⁴ J. Lueck,²⁷ P. Lujan,²⁹ P. Lukens,¹⁸ G. Lungu,⁵¹ J. Lys,²⁹ R. Lysak,¹⁵ D. MacQueen,³⁴ R. Madrak,¹⁸ K. Maeshima,¹⁸ K. Makhoul,³³ P. Maksimovic,²⁶ S. Malde,⁴³ S. Malik,³¹ G. Manca^e,³⁰ A. Manousakis-Katsikakis,³ F. Margaroli,⁴⁹ C. Marino,²⁷ C.P. Marino,²⁵ A. Martin,⁶¹ V. Martin^k,²² M. Martínez,⁴ R. Martínez-Ballarín,³² P. Mastrandrea,⁵² M. Mathis,²⁶ M.E. Mattson,⁵⁹ P. Mazzanti,⁶ K.S. McFarland,⁵⁰ P. McIntyre,⁵⁴ R. McNulty^j,³⁰ A. Mehta,³⁰ P. Mehtala,²⁴ A. Menzione,⁴⁷ C. Mesropian,⁵¹ T. Miao,¹⁸ D. Mietlicki,³⁵ N. Miladinovic,⁷ R. Miller,³⁶ C. Mills,²³ M. Milnik,²⁷ A. Mitra,¹ G. Mitselmakher,¹⁹ H. Miyake,⁵⁶ S. Moed,²³ N. Moggi,⁶ M.N. Mondragonⁿ,¹⁸ C.S. Moon,²⁸ R. Moore,¹⁸ M.J. Morello,⁴⁷ J. Morlock,²⁷ P. Movilla Fernandez,¹⁸ J. Mülmenstädt,²⁹ A. Mukherjee,¹⁸ Th. Muller,²⁷ P. Murat,¹⁸ M. Mussini^{cc},⁶ J. Nachtman^o,¹⁸ Y. Nagai,⁵⁶ J. Naganoma,⁵⁶ K. Nakamura,⁵⁶ I. Nakano,⁴¹ A. Napier,⁵⁷ J. Nett,⁶⁰ C. Neuz,⁴⁶ M.S. Neubauer,²⁵ S. Neubauer,²⁷ J. Nielsen^g,²⁹ L. Nodulman,² M. Norman,¹⁰ O. Norniella,²⁵ E. Nurse,³¹ L. Oakes,⁴³ S.H. Oh,¹⁷ Y.D. Oh,²⁸ I. Oksuzian,¹⁹ T. Okusawa,⁴² R. Orava,²⁴ K. Osterberg,²⁴ S. Pagan Griso^{dd},⁴⁴

C. Pagliarone,⁵⁵ E. Palencia,¹⁸ V. Papadimitriou,¹⁸ A. Papaikonomou,²⁷ A.A. Paramanov,² B. Parks,⁴⁰ S. Pashapour,³⁴ J. Patrick,¹⁸ G. Paulettaⁱⁱ,⁵⁵ M. Paulini,¹³ C. Paus,³³ T. Peiffer,²⁷ D.E. Pellett,⁸ A. Penzo,⁵⁵ T.J. Phillips,¹⁷ G. Piacentino,⁴⁷ E. Pianori,⁴⁶ L. Pinera,¹⁹ K. Pitts,²⁵ C. Plager,⁹ L. Pondrom,⁶⁰ K. Potamianos,⁴⁹ O. Poukhov^{*},¹⁶ F. Prokoshin^y,¹⁶ A. Pronko,¹⁸ F. Ptohosⁱ,¹⁸ E. Pueschel,¹³ G. Punzi^{ee},⁴⁷ J. Pursley,⁶⁰ J. Rademacker^c,⁴³ A. Rahaman,⁴⁸ V. Ramakrishnan,⁶⁰ N. Ranjan,⁴⁹ I. Redondo,³² P. Renton,⁴³ M. Renz,²⁷ M. Rescigno,⁵² S. Richter,²⁷ F. Rimondi^{cc},⁶ L. Ristori,⁴⁷ A. Robson,²² T. Rodrigo,¹² T. Rodriguez,⁴⁶ E. Rogers,²⁵ S. Rolli,⁵⁷ R. Roser,¹⁸ M. Rossi,⁵⁵ R. Rossin,¹¹ P. Roy,³⁴ A. Ruiz,¹² J. Russ,¹³ V. Rusu,¹⁸ B. Rutherford,¹⁸ H. Saarikko,²⁴ A. Safonov,⁵⁴ W.K. Sakumoto,⁵⁰ L. Santiⁱⁱ,⁵⁵ L. Sartori,⁴⁷ K. Sato,⁵⁶ A. Savoy-Navarro,⁴⁵ P. Schlabach,¹⁸ A. Schmidt,²⁷ E.E. Schmidt,¹⁸ M.A. Schmidt,¹⁴ M.P. Schmidt^{*},⁶¹ M. Schmitt,³⁹ T. Schwarz,⁸ L. Scodellaro,¹² A. Scribano^{ff},⁴⁷ F. Scuri,⁴⁷ A. Sedov,⁴⁹ S. Seidel,³⁸ Y. Seiya,⁴² A. Semenov,¹⁶ L. Sexton-Kennedy,¹⁸ F. Sforza^{ee},⁴⁷ A. Sfyrla,²⁵ S.Z. Shalhout,⁵⁹ T. Shears,³⁰ P.F. Shepard,⁴⁸ M. Shimojima^t,⁵⁶ S. Shiraishi,¹⁴ M. Shochet,¹⁴ Y. Shon,⁶⁰ I. Shreyber,³⁷ A. Simonenko,¹⁶ P. Sinervo,³⁴ A. Sisakyan,¹⁶ A.J. Slaughter,¹⁸ J. Slaunwhite,⁴⁰ K. Sliwa,⁵⁷ J.R. Smith,⁸ F.D. Snider,¹⁸ R. Snihur,³⁴ A. Soha,¹⁸ S. Somalwar,⁵³ V. Sorin,⁴ P. Squillacioti^{ff},⁴⁷ M. Stanitzki,⁶¹ R. St. Denis,²² B. Stelzer,³⁴ O. Stelzer-Chilton,³⁴ D. Stentz,³⁹ J. Strologas,³⁸ G.L. Strycker,³⁵ J.S. Suh,²⁸ A. Sukhanov,¹⁹ I. Suslov,¹⁶ A. Taffard^f,²⁵ R. Takashima,⁴¹ Y. Takeuchi,⁵⁶ R. Tanaka,⁴¹ J. Tang,¹⁴ M. Tecchio,³⁵ P.K. Teng,¹ J. Thom^h,¹⁸ J. Thome,¹³ G.A. Thompson,²⁵ E. Thomson,⁴⁶ P. Tipton,⁶¹ P. Ttito-Guzmán,³² S. Tkaczyk,¹⁸ D. Toback,⁵⁴ S. Tokar,¹⁵ K. Tollefson,³⁶ T. Tomura,⁵⁶ D. Tonelli,¹⁸ S. Torre,²⁰ D. Torretta,¹⁸ P. Totaroⁱⁱ,⁵⁵ S. Tourneur,⁴⁵ M. Trovato^{gg},⁴⁷ S.-Y. Tsai,¹ Y. Tu,⁴⁶ N. Turini^{ff},⁴⁷ F. Ukegawa,⁵⁶ S. Uozumi,²⁸ N. van Remortel^b,²⁴ A. Varganov,³⁵ E. Vataga^{gg},⁴⁷ F. Vázquezⁿ,¹⁹ G. Velev,¹⁸ C. Vellidis,³ M. Vidal,³² I. Vila,¹² R. Vilar,¹² M. Vogel,³⁸ I. Volobouev^w,²⁹ G. Volpi^{ee},⁴⁷ P. Wagner,⁴⁶ R.G. Wagner,² R.L. Wagner,¹⁸ W. Wagner^{aa},²⁷ J. Wagner-Kuhr,²⁷ T. Wakisaka,⁴² R. Wallny,⁹ S.M. Wang,¹ A. Warburton,³⁴ D. Waters,³¹ M. Weinberger,⁵⁴ J. Weinel^t,²⁷ W.C. Wester III,¹⁸ B. Whitehouse,⁵⁷ D. Whiteson^f,⁴⁶ A.B. Wicklund,² E. Wicklund,¹⁸ S. Wilbur,¹⁴ G. Williams,³⁴ H.H. Williams,⁴⁶ P. Wilson,¹⁸ B.L. Winer,⁴⁰ P. Wittich^h,¹⁸ S. Wolbers,¹⁸ C. Wolfe,¹⁴ H. Wolfe,⁴⁰ T. Wright,³⁵ X. Wu,²¹ F. Würthwein,¹⁰ A. Yagil,¹⁰ K. Yamamoto,⁴² J. Yamaoka,¹⁷ U.K. Yang^r,¹⁴ Y.C. Yang,²⁸ W.M. Yao,²⁹ G.P. Yeh,¹⁸ K. Yi^o,¹⁸ J. Yoh,¹⁸ K. Yorita,⁵⁸ T. Yoshida^l,⁴² G.B. Yu,¹⁷ I. Yu,²⁸ S.S. Yu,¹⁸ J.C. Yun,¹⁸ A. Zanetti,⁵⁵ Y. Zeng,¹⁷ X. Zhang,²⁵ Y. Zheng^d,⁹ and S. Zucchelli^{cc6}

(CDF Collaboration[†])

¹*Institute of Physics, Academia Sinica, Taipei, Taiwan 11529, Republic of China*

²*Argonne National Laboratory, Argonne, Illinois 60439*

³*University of Athens, 157 71 Athens, Greece*

⁴*Institut de Fisica d'Altes Energies, Universitat Autònoma de Barcelona, E-08193, Bellaterra (Barcelona), Spain*

⁵*Baylor University, Waco, Texas 76798*

⁶*Istituto Nazionale di Fisica Nucleare Bologna, ^{cc}University of Bologna, I-40127 Bologna, Italy*

⁷*Brandeis University, Waltham, Massachusetts 02254*

⁸*University of California, Davis, Davis, California 95616*

⁹*University of California, Los Angeles, Los Angeles, California 90024*

¹⁰*University of California, San Diego, La Jolla, California 92093*

¹¹*University of California, Santa Barbara, Santa Barbara, California 93106*

¹²*Instituto de Fisica de Cantabria, CSIC-University of Cantabria, 39005 Santander, Spain*

¹³*Carnegie Mellon University, Pittsburgh, PA 15213*

¹⁴*Enrico Fermi Institute, University of Chicago, Chicago, Illinois 60637*

¹⁵*Comenius University, 842 48 Bratislava, Slovakia; Institute of Experimental Physics, 040 01 Kosice, Slovakia*

¹⁶*Joint Institute for Nuclear Research, RU-141980 Dubna, Russia*

¹⁷*Duke University, Durham, North Carolina 27708*

¹⁸*Fermi National Accelerator Laboratory, Batavia, Illinois 60510*

¹⁹*University of Florida, Gainesville, Florida 32611*

²⁰*Laboratori Nazionali di Frascati, Istituto Nazionale di Fisica Nucleare, I-00044 Frascati, Italy*

²¹*University of Geneva, CH-1211 Geneva 4, Switzerland*

²²*Glasgow University, Glasgow G12 8QQ, United Kingdom*

²³*Harvard University, Cambridge, Massachusetts 02138*

²⁴*Division of High Energy Physics, Department of Physics,*

University of Helsinki and Helsinki Institute of Physics, FIN-00014, Helsinki, Finland

²⁵*University of Illinois, Urbana, Illinois 61801*

²⁶*The Johns Hopkins University, Baltimore, Maryland 21218*

²⁷*Institut für Experimentelle Kernphysik, Karlsruhe Institute of Technology, D-76131 Karlsruhe, Germany*

²⁸*Center for High Energy Physics: Kyungpook National University,*

Daegu 702-701, Korea; Seoul National University, Seoul 151-742,

Korea; Sungkyunkwan University, Suwon 440-746,

- Korea; Korea Institute of Science and Technology Information,
Daejeon 305-806, Korea; Chonnam National University, Gwangju 500-757,
Korea; Chonbuk National University, Jeonju 561-756, Korea
- ²⁹Ernest Orlando Lawrence Berkeley National Laboratory, Berkeley, California 94720
- ³⁰University of Liverpool, Liverpool L69 7ZE, United Kingdom
- ³¹University College London, London WC1E 6BT, United Kingdom
- ³²Centro de Investigaciones Energeticas Medioambientales y Tecnologicas, E-28040 Madrid, Spain
- ³³Massachusetts Institute of Technology, Cambridge, Massachusetts 02139
- ³⁴Institute of Particle Physics: McGill University, Montréal, Québec,
Canada H3A 2T8; Simon Fraser University, Burnaby, British Columbia,
Canada V5A 1S6; University of Toronto, Toronto, Ontario,
Canada M5S 1A7; and TRIUMF, Vancouver, British Columbia, Canada V6T 2A3
- ³⁵University of Michigan, Ann Arbor, Michigan 48109
- ³⁶Michigan State University, East Lansing, Michigan 48824
- ³⁷Institution for Theoretical and Experimental Physics, ITEP, Moscow 117259, Russia
- ³⁸University of New Mexico, Albuquerque, New Mexico 87131
- ³⁹Northwestern University, Evanston, Illinois 60208
- ⁴⁰The Ohio State University, Columbus, Ohio 43210
- ⁴¹Okayama University, Okayama 700-8530, Japan
- ⁴²Osaka City University, Osaka 588, Japan
- ⁴³University of Oxford, Oxford OX1 3RH, United Kingdom
- ⁴⁴Istituto Nazionale di Fisica Nucleare, Sezione di Padova-Trento, ^{4d}University of Padova, I-35131 Padova, Italy
- ⁴⁵LPNHE, Université Pierre et Marie Curie/IN2P3-CNRS, UMR7585, Paris, F-75252 France
- ⁴⁶University of Pennsylvania, Philadelphia, Pennsylvania 19104
- ⁴⁷Istituto Nazionale di Fisica Nucleare Pisa, ^{4e}University of Pisa,
^{4f}University of Siena and ^{4g}Scuola Normale Superiore, I-56127 Pisa, Italy
- ⁴⁸University of Pittsburgh, Pittsburgh, Pennsylvania 15260
- ⁴⁹Purdue University, West Lafayette, Indiana 47907
- ⁵⁰University of Rochester, Rochester, New York 14627
- ⁵¹The Rockefeller University, New York, New York 10021
- ⁵²Istituto Nazionale di Fisica Nucleare, Sezione di Roma 1,
^{5h}Sapienza Università di Roma, I-00185 Roma, Italy
- ⁵³Rutgers University, Piscataway, New Jersey 08855
- ⁵⁴Texas A&M University, College Station, Texas 77843
- ⁵⁵Istituto Nazionale di Fisica Nucleare Trieste/Udine,
I-34100 Trieste, ⁵ⁱUniversity of Trieste/Udine, I-33100 Udine, Italy
- ⁵⁶University of Tsukuba, Tsukuba, Ibaraki 305, Japan
- ⁵⁷Tufts University, Medford, Massachusetts 02155
- ⁵⁸Waseda University, Tokyo 169, Japan
- ⁵⁹Wayne State University, Detroit, Michigan 48201
- ⁶⁰University of Wisconsin, Madison, Wisconsin 53706
- ⁶¹Yale University, New Haven, Connecticut 06520

The cross section for photon production in association with at least one jet containing a b -quark hadron has been measured in proton antiproton collisions at $\sqrt{s} = 1.96$ TeV. The analysis uses a data sample corresponding to an integrated luminosity of 340 pb^{-1} collected with the CDF II detector. Both the differential cross section as a function of photon transverse energy E_T^γ , $d\sigma(p\bar{p} \rightarrow \gamma + \geq 1b\text{-jet})/dE_T^\gamma$ and the total cross section $\sigma(p\bar{p} \rightarrow \gamma + \geq 1b\text{-jet}; E_T^\gamma > 20 \text{ GeV})$ are measured. Comparisons to a next-to-leading order prediction of the process are presented.

PACS numbers: Valid PACS appear here

*Deceased

†With visitors from ^aUniversity of Massachusetts Amherst, Amherst, Massachusetts 01003, ^bUniversiteit Antwerpen, B-2610 Antwerp, Belgium, ^cUniversity of Bristol, Bristol BS8 1TL, United Kingdom, ^dChinese Academy of Sciences, Beijing 100864, China, ^eIstituto Nazionale di Fisica Nucleare, Sezione di Cagliari, 09042 Monserrato (Cagliari), Italy, ^fUniversity of California Irvine, Irvine, CA 92697, ^gUniversity of California Santa Cruz, Santa Cruz, CA 95064, ^hCornell University, Ithaca, NY 14853,

ⁱUniversity of Cyprus, Nicosia CY-1678, Cyprus, ^jUniversity College Dublin, Dublin 4, Ireland, ^kUniversity of Edinburgh, Edinburgh EH9 3JZ, United Kingdom, ^lUniversity of Fukui, Fukui City, Fukui Prefecture, Japan 910-0017 ^mKinki University, Higashi-Osaka City, Japan 577-8502 ⁿUniversidad Iberoamericana, Mexico D.F., Mexico, ^oUniversity of Iowa, Iowa City, IA 52242, ^pKansas State University, Manhattan, KS 66506 ^qQueen Mary, University of London, London, E1 4NS, England, ^rUniversity of Manch-

The study of proton-antiproton interactions with an isolated, high energy photon and an identified b -quark jet is a testing ground for quantum chromodynamics (QCD) predictions at the Tevatron. At photon transverse energies E_T^γ below 70 GeV Compton scattering processes dominate production, with $gb \rightarrow \gamma gb$ or $qb \rightarrow \gamma qb$ dominating at lower E_T^γ depending on the relative sizes of the quark and gluon parton density functions. Above an E_T^γ of 70 GeV $q\bar{q} \rightarrow b\bar{b}\gamma$ quark annihilation processes dominate production [1]. A cross section measurement therefore provides a well measured probe of the hard scattering dynamics within the proton, and some sensitivity to the b -quark content of the proton, whose parton density function is so far indirectly extracted from constraints on the gluon density functions.

The first measurement of photon and heavy flavour jet production was performed using 86 pb^{-1} of integrated luminosity taken at $\sqrt{s} = 1.8 \text{ TeV}$ with the CDF I detector [2]. Heavy jet flavor was signalled by muons contained in the jet. The results were interpreted in terms of new physics processes involving the radiative decay of Techni-Omega states [3], and radiative decays of supersymmetric particles in gauge-mediated supersymmetry models [4]. Recently the D0 collaboration has measured the cross section of heavy flavour jet production in association with a photon [5] using data collected at $\sqrt{s} = 1.96 \text{ TeV}$. In this paper we exploit improvements in the CDF II detector to identify b jets by a lifetime based secondary vertex tag, use a larger dataset collected at a higher center-of-mass energy, probe lower photon transverse energy, and employ a superior analysis technique where all backgrounds are determined directly from data. We present our results as the differential photon + b jet production cross section, as a function of photon E_T^γ , and the total photon + b jet production cross section.

The CDF II detector is described in detail in [6]. Only the components which are most relevant to this analysis will be described here.

The detector is composed of a central spectrometer inside a 1.4T magnetic field, surrounded by electromagnetic and hadronic calorimetry and muon chambers. The spectrometer is composed of a multi-layer silicon vertex detector inside a cylindrical multi-wire drift chamber. The combination of these tracking detectors measures charged particle trajectories with a transverse momentum (p_T)

precision of $\Delta p_T/p_T^2 = 0.07\% (\text{GeV}/c)^{-1}$, and an uncertainty on the transverse impact parameter of about $40 \mu\text{m}$ for tracks of p_T above $1 \text{ GeV}/c$, which includes the intrinsic beam size of about $30 \mu\text{m}$. Information from the central tracker can be sent within trigger latency to the hardware tracker SVT[7], that provides an extra-fast measurement of the tracking parameters that can be used at trigger level.

Segmented sampling calorimeters, arranged in a projective tower geometry, surround the tracking detectors and provide energy measurements within the region $|\eta| < 3.6$. Central calorimeters [8] cover the region $|\eta| < 1.1$, with an electromagnetic (hadronic) energy resolution of $\sigma(E)/E = 13.5\%/\sqrt{E} \oplus 2.0\%$ ($\sigma(E)/E = 50\%/\sqrt{E_T} \oplus 3\%$). The end-wall hadronic calorimeter extends this coverage to $|\eta| < 1.3$ [9] with an energy resolution of $75\%/\sqrt{E_T} \oplus 4\%$, whilst the region $1.3 < |\eta| < 3.6$ ($1.1 < |\eta| < 3.6$ for the electromagnetic calorimeter) is covered by forward calorimeters [10], with hadronic and electromagnetic energy resolutions of $80\%/\sqrt{E} \oplus 5\%$ and $16\%/\sqrt{E} \oplus 1\%$ respectively. In order to distinguish electromagnetic clusters from photons and electrons, and clusters from neutral pion decays, the central electromagnetic calorimeter is equipped with two sets of wire chambers: a preshower detector (CPR) situated in front of the active part of the calorimeter to detect early photon conversions in the solenoid coil, and a shower maximum detector (CES) placed at the position of maximal width of electromagnetic showers to measure the shower profile. Signals from these detectors are compared with expected deposits from electromagnetic clusters, obtained from testbeam data. Each electromagnetic cluster is given a weight related to the probability that it originates from a photon.

We use data obtained by two triggers; a trigger which requires a photon-like object with transverse energy larger than the threshold for the inclusive photon trigger at CDF of 25 GeV ('high E_T^γ photon'), and a trigger ('SVT photon') which requires a photon-like object with transverse energy larger than 12 GeV, a jet with transverse energy larger than 10 GeV, and a track, measured by the SVT [7], with transverse momentum larger than $2 \text{ GeV}/c$, an absolute rapidity smaller than 1 and an impact parameter larger than $120 \mu\text{m}$. The SVT compares hits from the tracking detectors with pre-fitted tracks stored in an associative memory to extract track parameters in real time. In this way tracks with significant impact parameters can be quickly identified. The impact parameter resolution of this procedure is less than $50 \mu\text{m}$ (including the contribution from the beam size), similar to the accuracy obtained with full detector reconstruction. An integrated luminosity of $340 (208) \text{ pb}^{-1}$ of data has been analyzed in the high E_T^γ photon (SVT photon) triggered dataset.

The two triggers have very different efficiencies. The high E_T^γ photon trigger has an efficiency close to 100% for events with E_T^γ above 28 GeV. To obtain photons of lower E_T^γ the SVT trigger must be used. The efficiency

ester, Manchester M13 9PL, England, ^{*}Muons, Inc., Batavia, IL 60510, [†]Nagasaki Institute of Applied Science, Nagasaki, Japan, [‡]University of Notre Dame, Notre Dame, IN 46556, [§]University de Oviedo, E-33007 Oviedo, Spain, ^{||}Texas Tech University, Lubbock, TX 79609, [¶]IFIC(CSIC-Universitat de Valencia), 56071 Valencia, Spain, [⊖]Universidad Tecnica Federico Santa Maria, 110v Valparaiso, Chile, [⊗]University of Virginia, Charlottesville, VA 22906 [⊕]Bergische Universität Wuppertal, 42097 Wuppertal, Germany, [⊘]Yarmouk University, Irbid 211-63, Jordan [⊙]On leave from J. Stefan Institute, Ljubljana, Slovenia,

of the SVT photon trigger is found by comparing the number of events that pass both triggers. Being based on strong requirements on a single track rather than a more refined secondary vertex reconstruction, the efficiency of the SVT-based photon trigger is about 50% (with a relative uncertainty of 4%, due to the size of the overlap sample) and was found to be independent of the jet transverse energy.

Selected candidate events must pass one of the two photon triggers, contain an isolated central ($|\eta| < 1.1$) photon of $E_T^\gamma > 20$ GeV, and a b jet of $E_T > 20$ GeV within $|\eta| < 1.5$.

Photon candidates must have a calorimeter cluster which contains predominately electromagnetic energy. The cluster hadronic energy fraction E_{HAD}/E_{EM} must satisfy $E_{HAD}/E_{EM} < 0.055 + 0.00045 * E^\gamma$, where E^γ is the photon energy and E_{HAD} and E_{EM} are the hadronic and electromagnetic energy deposits within the cluster. The electromagnetic shower profile must also agree with that expected for an electromagnetic deposit. In order to reduce contamination from neutral meson (such as π^0) decays, photon candidates must be isolated from nearby calorimetric deposits and tracks. We require that $E_T(R^{0.4}) < 2.0 + 0.02(E_T^\gamma - 20)$, where $E_T(R^{0.4})$ is the summed calorimetric cluster transverse energy deposits in a cone of radius $R = \sqrt{\Delta\phi^2 + \Delta\eta^2} = 0.4$ around the photon candidate, to ensure calorimetric isolation. In addition, the summed track transverse momenta of tracks inside this cone, $p_T(R^{0.4})$ must satisfy $p_T(R^{0.4}) < 2.0 + E_T^\gamma * 0.005$ to ensure isolation in the tracking detectors. Events containing adjacent calorimetric clusters in the CES, which can signal the presence of neutral mesons, are rejected.

The jets in each event are reconstructed using the JET-CLU algorithm [11] with cone radius $R = 0.4$ (0.7) for events containing photons of $E_T^\gamma < (>)26$ GeV. To recover the true parton energy, jets are corrected for instrumental effects [12]. We select events containing at least one jet with corrected $E_T > 20$ GeV, and whose axis lies outside a cone of $\Delta R = 0.7$ surrounding the photon candidate. In order to identify jets arising from b hadrons we search for displaced secondary vertices [13]. A b jet is identified ('tagged') when the secondary vertex is more than two standard deviations away from the beam position, and in the same direction away from the beam position as the jet momentum. We require at least one b jet to be identified in each event. The efficiency of the b-tagging algorithm is just under 25% for b jets of $E_T = 20$ GeV, and increases to 40% at $E_T = 50$ GeV.

The PYTHIA [14] Monte Carlo code is used to simulate photon + jet production at leading order and to estimate the photon and jet selection efficiencies. The Q^2 scale of the interaction is set to 225 GeV², and the CTEQ5L [15] parton distribution functions are used. A simulation of the underlying event is included [16].

Backgrounds to photons arise from high energy π^0 's, which decay to pairs of overlapping photons that cannot be distinguished in the calorimeter, but whose rate

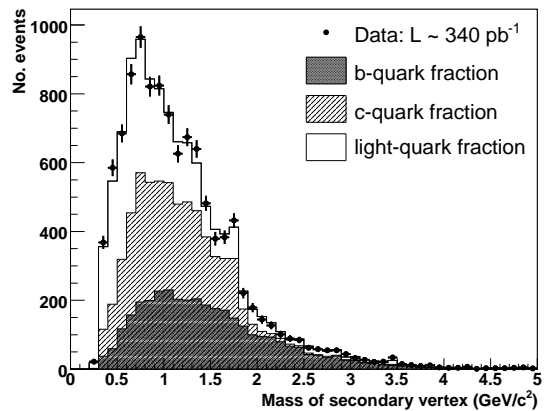


FIG. 1: Fit to the invariant mass of tracks composing the secondary vertex in data, for photon candidates having $E_T > 26$ GeV. The points are data, and the stacked, shaded histograms represent the estimated contributions of the b-, c- and light-quark jets.

can be estimated directly from the data. The fraction of misidentified photons is estimated using the clusters detected by the CPR and CES detectors of the electromagnetic calorimeter. Photon pairs produced by π^0 decays will produce a larger number of hits in these detectors, and each photon candidate is assigned a weight proportional to the probability of being a signal or background cluster following the procedure detailed in [17]. The fraction of correctly identified photons in the sample passing those selection criteria increases with increasing E_T , going from about 50% at the lower end of the spectrum considered here (20 GeV) to around 80% at high E_T^γ . Backgrounds to b jets can arise from jets originating from charm quarks, since charm hadrons have a lifetime between a quarter and two thirds that of b-hadrons, and jets originating from light quarks and gluons, where random combinations of tracks can sometimes mimic a vertex displaced from the beamline. The purity of our selected events is determined by fitting the invariant mass of tracks composing the secondary vertex in data to Monte Carlo templates of the shapes expected for b-, charm (c-) and light-quark jets. Fig. 1 shows an example of the fit to data. Here, about a third of jets arise from b quarks. This invariant mass is generally lower than the corresponding hadron mass due to mis-assigned tracks and unreconstructed neutral hadrons. It can be seen that the template shapes of the different quark jet types are sufficiently different to provide reasonable discriminating power.

Identified b jets can arise from either the photon + b jet signal, or from events where one or both objects (photon and jet) are mis-identified. We assume that the tagged jet composition in $\pi^0 +$ tagged jet events is similar to $\pi^\pm +$ tagged jet events. We estimate the b jet purity of the misidentified photon background using data collected with a jet based trigger. Events are required to contain two jets, one of which must be tagged and have similar transverse energy and pseudorapidity requirements

to the b jet, and a second which passes similar kinematic requirements to the photon. The fraction of b jets in this sample can be found by fitting the secondary vertex invariant mass of the tagged jets. The purity of the selected jets ranges from 50% for jets of E_T around 20 GeV, to about 15% for jets of E_T around 75 GeV where the rate of light-quark jet tagging increases. This b fraction is then normalised to the estimated number of misidentified photons, and subtracted from the estimated number of b jets in the whole event sample to yield the total number of photon + b jet events.

Some 10900 (55800) events pass the selection criteria in the high transverse energy photon (SVT photon) triggered datasets. Candidate events are divided into bins of photon transverse energy. The numbers of events in each bin are corrected for background contributions, trigger, selection and acceptance efficiency, and divided by the appropriate integrated luminosity to yield a cross section. Results are given in Table I, which also lists the systematic uncertainties detailed later. Note that the statistical uncertainty for the high E_T^γ photon dataset includes contributions from finite Monte Carlo statistics.

Several sources of systematic uncertainty in the cross section determination have been studied: photon identification, jet energy scale, b jet identification, and luminosity. In the following only the largest contributions will be quantified.

Variables used in photon identification have been studied in $Z \rightarrow e^+e^-$ simulation and data events [18]. Simulation and data are consistent. Uncertainties in the misidentified photon estimate arise from assumed values for the preshower detector hit rate, the rate of backscattered showers and the fractional composition of fake photon backgrounds. The associated systematic uncertainty is about 6%.

The systematic uncertainty on the jet energy scale has been studied in detail elsewhere [12] and the findings applied to this analysis. It decreases with increasing jet E_T , and is about 5% for jets of 35 GeV E_T . Uncertainties have also been determined for the effect of multiple interactions overlapping in the same data event, and the additional uncertainty on the jet scale introduced by a b jet.

Uncertainties in the b quark purity of the sample arise from imperfect modelling of the template shapes used in fits to extract the b purity. Differences in shape can arise if the secondary vertex invariant mass of jets containing one ('single') or two ('double') b quarks differs, or if track efficiency is incorrectly modelled. We find that template shapes obtained from single and double quark jets are not consistent with each other. The data are fitted to templates composed of mixtures of the individual single and double quark templates (ranging from 0 to 100%), and the χ^2 of the resulting distributions with respect to the data is computed. We take as a $1 - \sigma$ deviation the value for this mixture for which the χ^2 increases by one unit with respect to its minimum value, and recalculate the cross section using this mixed template. The systematic

uncertainty is the difference between this value and the default cross section (obtained with the default diquark fraction).

The uncertainty on the cross section is assigned as the difference between the reference value and that obtained from the value of the single/double quark template for which the χ^2 increases by one unit with respect to its minimum value. This is the largest single source of uncertainty and is about 17%. Previous studies [19] suggest a difference in tracking efficiency between data and simulation which is a function of isolation, momentum, and position in the detector. We remake the invariant mass templates incorporating the inefficiency derived from data, and take the full difference between results obtained using these and the nominal templates (5%) as the systematic uncertainty due to this source.

Other systematic uncertainties on b jet identification arise from the difference in measured tagging efficiency between data and simulation, from the difference in the tagging efficiency of single and double b jets, and from simulated b hadron multiplicity. The first uncertainty has been previously studied [13]. The difference in scale between tagging efficiency in data and simulation was found to be 0.91 ± 0.06 . This results in a 6% uncertainty on the measured cross-sections. The uncertainty on tagging efficiency for single and double b jets is determined as the difference between results obtained using the fractions of single and double quark templates corresponding to ± 1 standard deviation, as found earlier, and is about 7%. We have adopted the findings of previous studies of the effect of assumed b hadron multiplicity [19] (a 1% effect on the measured cross section). The SVT-based analysis is also affected by the statistical precision of the trigger efficiency determination (about 10%). Finally, the luminosity is subject to a $\pm 6\%$ uncertainty [20].

The cross section for photons produced in association with b jets is tabulated in Table I. Both differential and inclusive results are given, with their statistical and systematic uncertainties. Note that results from both datasets are listed. There is overlap between the final SVT photon and the first high E_T^γ photon bins, which give consistent results. Due to its greater statistical precision, the former bin is used in the final results. The measurements are corrected to hadron level [21], so that they can be directly compared to a recent next-to-leading order calculation[1]. This prediction was derived analytically, using the CTEQ6.6M parton density functions [22], and a renormalisation, factorisation and fragmentation scale set to the transverse momentum of the photon. It does not include non-perturbative effects (hadronisation and underlying event), and is presented in terms of parton level jets.

The measured cross sections are shown compared with this prediction in Fig. 2. Also shown are the theoretical uncertainties due to (i) choice of scale and (ii) uncertainty in parton density function assumption. Agreement with next-to-leading order theory is good over the entire photon E_T^γ range probed. It should be noted that due

E_T^γ (GeV)	$d\sigma(p\bar{p} \rightarrow \gamma + \geq 1b\text{-jet})/dE_T^\gamma(\text{Data})$	$d\sigma(p\bar{p} \rightarrow \gamma + \geq 1b\text{-jet})/dE_T^\gamma(\text{NLO})$
20 - 24	$3.90 \pm 0.49 \pm 0.84$	3.27 ± 0.78
24 - 28	$3.01 \pm 0.41 \pm 0.63$	3.67 ± 0.32
26 - 28(*)	$3.13 \pm 0.51 \pm 0.67$	3.01 ± 0.21
28 - 31	$2.90 \pm 0.42 \pm 0.61$	2.65 ± 0.18
31 - 35	$1.24 \pm 0.20 \pm 0.27$	1.72 ± 0.14
35 - 43	$0.94 \pm 0.14^{+0.18}_{-0.20}$	0.92 ± 0.10
43 - 70	$0.20 \pm 0.03 \pm 0.04$	0.21 ± 0.05

TABLE I: The measured differential cross section for central photon production in association with at least one b -jet of $E_T > 20$ GeV, inside $|\eta| < 1.5$, tabulated as a function of the photon transverse energy E_T^γ . The first (second) uncertainty quoted is statistical (systematic). Results are compared to a next-to-leading order (NLO) prediction, whose uncertainty arises from the numerical integration procedure [1]. Note that the first two measurements are made using the SVT dataset, and the remainder with the high E_T^γ dataset. The overlap bin, denoted by (*), is not used in the final results. Systematics about luminosity, secondary vertex tagging scale factor, the effect of multiple vertices are correlated between all bins. The uncertainty due to the statistical precision of the SVT trigger efficiency is fully correlated between the first two bins only. All other uncertainties are uncorrelated between bins.

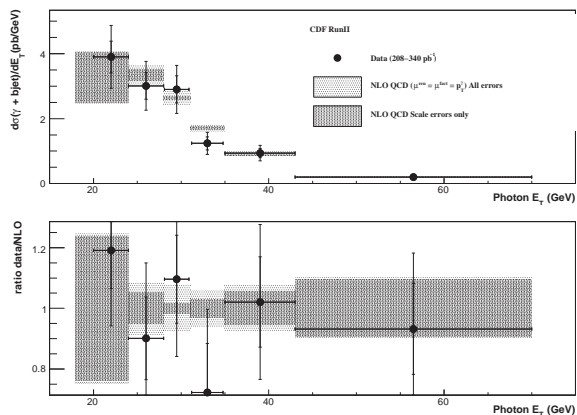


FIG. 2: Top: b + photon cross section as a function of photon E_T , compared to NLO QCD calculations. The light dashed is a quadrature sum of uncertainties coming from scale variation (both renormalisation and factorisation scales varied by a factor 2 and 0.5) and PDFs, while the darker dashed represents the scale variation contribution only. The inner error bars for data represent the statistical uncertainties, the outer the combination of statistical and systematic. The bottom plot shows the ratio of data to NLO calculation, where the error bars and shading have the same meaning as before.

to numerical stability problems, the first bin in the NLO calculation starts at 18 GeV instead of 20 as for the data.

The total cross section $\sigma(p\bar{p} \rightarrow \gamma + \geq 1b\text{-jet}; E_T^\gamma > 20$ GeV) has been measured to be 54.22 ± 3.26 (stat) $^{+5.04}_{-5.09}$ (syst) pb. This is consistent with the next-to-leading order prediction of 55.62 ± 3.87 pb.

In conclusion, the cross section for photon production

in association with b jets has been measured in proton antiproton collisions at $\sqrt{s} = 1.96$ TeV with the CDF II detector. The measurement has been made for b -jets with $E_T > 20$ GeV inside $|\eta| < 1.5$, and for photons of at least $E_T^\gamma > 20$ GeV inside $|\eta| < 1.1$, including the lowest photon transverse energies probed to date. The results are consistent with next-to-leading order theoretical perturbative QCD predictions, using CTEQ6.6M parton density functions, throughout the photon E_T^γ range measured, while leading-order calculations would predict a cross section smaller by about 30%. The level of accuracy of this measurement is therefore already sufficient to discriminate between the first orders of perturbative expansion, and favor the most precise NLO predictions.

We thank the Fermilab staff and the technical staffs of the participating institutions for their vital contributions. This work was supported by the U.S. Department of Energy and National Science Foundation; the Italian Istituto Nazionale di Fisica Nucleare; the Ministry of Education, Culture, Sports, Science and Technology of Japan; the Natural Sciences and Engineering Research Council of Canada; the National Science Council of the Republic of China; the Swiss National Science Foundation; the A.P. Sloan Foundation; the Bundesministerium für Bildung und Forschung, Germany; the World Class University Program, the National Research Foundation of Korea; the Science and Technology Facilities Council and the Royal Society, UK; the Institut National de Physique Nucleaire et Physique des Particules/CNRS; the Russian Foundation for Basic Research; the Ministerio de Ciencia e Innovación, and Programa Consolider-Ingenio 2010, Spain; the Slovak R&D Agency; and the Academy of Finland.

[1] T.Stavreva and J.Owens, Phys. Rev. D **79**, 054017 (2009), and private communication relating predictions

to the kinematic requirements used in the analysis presented here.

- [2] T. Affolder *et al.* (CDF Collaboration), Phys. Rev. D **65**, 052006 (2002)
- [3] F. Abe *et al.* (CDF Collaboration), Phys. Rev. D **60**, 092003 (1999).
- [4] T. Affolder *et al.* (CDF Collaboration), Phys. Rev. D **65**, 052006 (2002).
- [5] V. M. Abazov *et al.* (D0 Collaboration), Phys. Rev. Lett. **102**, 192002 (2009).
- [6] CDF Collaboration, FERMILAB-PUB-96/390-E, 1996, and Phys. Rev. D **68**, 072004 (2003).
- [7] W. Ashmanskas *et al.*, Nucl. Instrum. Methods A **447**, 218 (2000).
- [8] L. Balka *et al.*, Nucl. Instrum. Methods A **267**, 272 (1988).
- [9] S. Bertolucci *et al.*, Nucl. Instrum. Methods A **267**, 301 (1988).
- [10] R. Oishi, Nucl. Instrum. Methods A **453**, 277 (2000); M. G. Albrow *et al.*, Nucl. Instrum. Methods A **480**, 524 (2002).
- [11] F. Abe *et al.* (CDF Collaboration), Phys. Rev. D **45**, 1448 (1992).
- [12] A. Bhatti *et al.*, Nucl. Instrum. Methods A **566**, 2 (2006).
- [13] D. Acosta *et al.* (CDF Collaboration), Phys. Rev. D **71**, 052003 (2005).
- [14] T. Sjostrand *et al.*, JHEP 05, 026 (2006).
- [15] H. L. Lai *et al.*, Eur. Phys. J. C **12**, 375 (2000).
- [16] R. Field, AIP Conf. Proc. 828:163 (2006).
- [17] F. Abe *et al.* (CDF Collaboration), Phys. Rev. D **48**, 2998 (1993).
- [18] D. Acosta *et al.* (CDF Collaboration), Phys. Rev. Lett. **95**, 022003 (2005).
- [19] A. Abulencia *et al.* (CDF Collaboration), Phys. Rev. D **74**, 032008 (2006).
- [20] S. Klimenko, J. Konigsberg, T. M. Liss, *FERMILAB-FN-0741* (2003).
- [21] The hadron level in Monte Carlo generators is defined using all final state particles with lifetime above 10^{-11} s.
- [22] P. M. Nadolsky, Phys. Rev. D **78**, 013004 (2008).